



## Section 7. Material erosion

**Erosion behavior and surface characterization of beryllium under high-flux deuterium plasma bombardment**J. Won <sup>a,\*</sup>, F.E. Spada <sup>b</sup>, R. Boivin <sup>a</sup>, R. Doerner <sup>a</sup>, S Luckhardt <sup>a</sup>, F.C. Sze <sup>a</sup>, R.W. Conn <sup>a</sup><sup>a</sup> Fusion Energy Research Program, Mechanical Engineering Division, University of California at San Diego, La Jolla, CA 92093, USA<sup>b</sup> Center for Magnetic Recording Research, University of California at San Diego, La Jolla, CA 92093, USA**Abstract**

The erosion of beryllium subject to a high-flux deuterium plasma is studied, including post-bombardment surface characterization. Simulating divertor plasma conditions of the ITER tokamak, the PISCES-B steady-state plasma facility at U.C., San Diego is used to bombard beryllium specimens. The measured sputtering yield is compared with theoretical Monte Carlo calculations using the TRIM.SP code, and with experimental values obtained by others using an ion beam facility. It is found that at elevated specimen temperatures ( $250^{\circ}\text{C} \leq T \leq 720^{\circ}\text{C}$ ), low atomic number impurities of the plasma, such as carbon, nitrogen, and oxygen, form an impurity layer on the beryllium surface. This layer is not eroded away by extended plasma exposure but appears to be continuously regenerated. The presence of this film reduces the apparent sputtering yield of beryllium by up to two orders of magnitude. An in-situ emission spectroscopy technique is used to confirm the effect of deposited contaminants. Depth-profile Auger electron spectroscopy (AES) data shows that relative concentration of carbon, nitrogen, and oxygen in the thin film is each in the range, 10 to 20%. X-ray photoelectron spectroscopy (XPS) data indicates the formation of BeO and a small amount of Be<sub>2</sub>C on the surface. X-ray diffraction (XRD) patterns obtained with a small angle of incidence show no evidence for crystalline Be<sub>2</sub>C and suggest that the impurity layer may have a disordered or amorphous structure. Importantly, no impurity deposition is observed when the specimen is maintained at room temperature ( $\sim 40^{\circ}\text{C}$ ). Application of energy dispersive X-ray spectroscopy (EDX) confirms that the low temperature surface is free of impurities except for a trace amount of oxygen. The sputtering yield measured at room temperature agrees with theoretical values within a factor of two.

**Keywords:** PISCES-B; Beryllium; Sputtering yield; Plasma-wall interaction simulator

**1. Introduction**

After the successful application as a plasma-facing material in the JET fusion experiments in 1991 [1], beryllium was chosen as the primary material for plasma-facing components in ITER [2]. However, the erosion behavior of beryllium when subjected to a strong plasma flux is not well understood. It is of crucial importance to know the sputtering yield of a plasma-facing material, because it

directly impacts the lifetime of the components. Initial measurements of the sputtering yield of beryllium in an ion beam device [3] were affected by a pre-existing surface oxide layer on the specimen. It is not known, however, if this thin oxide layer will remain on the surface under high-flux plasma bombardment conditions [4], where the bombarding particle fluxes are orders of magnitude higher than the ion beam fluxes. In this study, sputtering yield of beryllium is measured, for the first time, under low-energy, high-flux deuterium plasma bombardment conditions in the PISCES-B facility [5] using a weight loss method. Also, various surface analysis techniques are performed to characterize the plasma-bombarded beryllium.

\* Corresponding author. Tel.: +1-619 534 9740; fax: +1-619 534 7716; e-mail: jiwon@ucsd.edu.

## 2. Experiments

### 2.1. Sputtering yield

As-received S-65B beryllium manufactured by Brush Wellman Inc. is used for the measurement. It is a hot-pressed, powder metallurgy product with a purity of 99.0 wt% [6]. The nominal concentration of BeO is max. 1%. Argon ion beam etching data for a polished specimen indicates that the surface oxide layer thickness is about 15 nm. The diameter and thickness of specimens are 2.54 cm and 0.16 cm, respectively. The weight loss is measured within 5 min of air exposure following plasma bombardment. It is known that it takes 2 h air exposure at room temperature to reach a 10 nm thick oxide film [7], which approximately corresponds to 1.5  $\mu\text{g}$  of weight gain. Therefore, the air exposure will not affect the weight loss measurement. The measured weight loss in this study ranges from 0.15 mg to 2.6 mg.

The bombarding ion energy is controlled by biasing the specimen negatively. Plasma density and electron temperature are measured by a spatially-scanning double Langmuir probe. The plasma source is operated in an erosion regime to avoid redeposition [8]. The plasma density is varied from 0.1 to  $1.0 \times 10^{18} \text{ m}^{-3}$  and the electron temperature is set between 10 and 25 eV. The corresponding ion flux ranges from 0.2 to  $2.0 \times 10^{22} \text{ m}^{-2} \text{ s}^{-1}$  and the fluence ranges up to  $7.0 \times 10^{25} \text{ m}^{-2}$ . To study the effect of specimen temperature, we have measured the sputtering yield of beryllium both at elevated temperatures ( $250^\circ\text{C} \leq T \leq 720^\circ\text{C}$ ) and at room temperatures (around  $40^\circ\text{C}$ ). The specimen temperature is measured by two infrared pyrometers.

A line emission spectroscopy technique is used to study in situ erosion [9] of beryllium by monitoring the Be II line intensity. The fundamental resonance lines at 313.0 and 313.1 nm are the most intense transitions in the beryllium spectrum [10]. Since plasma parameters are maintained constant during the experiment, the line intensity is proportional to the number of sputtered beryllium atoms. A residual gas analyzer (RGA) is used to monitor partial pressures of residual gas species. The background pressure of the PISCES-B vacuum chamber is maintained around  $1.0 \times 10^{-7}$  Torr.

### 2.2. Surface morphology and analyses

Scanning electron microscope (SEM) pictures are taken before and after the deuterium plasma bombardment to study the morphology change. Depth-profile AES and XPS are performed for a specimen which is completely coated with a black film after plasma exposure. A 3 keV Ar ion beam, whose diameter is 0.4 mm, is raster-scanned to sputter-etch the specimen surface for four hours. The crystalline structure of the impurity layer formed on beryllium surface during plasma exposure is investigated by

XRD using asymmetric geometry. A Co K $\alpha$  line ( $\lambda = 1.790 \text{ \AA}$ ) is held fixed at a small incident angle to enhance diffraction from the specimen surface.

## 3. Results and discussion

### 3.1. Sputtering yield

Bohdansky and Roth [3] found that, at a deuterium ion energy of 100 eV, the sputtering yield of beryllium at an elevated temperature was three times larger than the values at room temperature. This enhanced sputtering yield at a high temperature was explained as being the result of beryllium diffusing through the oxide layer and subsequently being sputtered from the surface. However, the opposite is observed in the PISCES-B experiments. Namely, the measured sputtering yield of beryllium at elevated temperatures is lower than that at room temperature, as shown in Fig. 1. In the figure, the apparent sputtering yield of beryllium measured in PISCES-B is plotted as a function of the deuterium ion energy for room temperature ( $\sim 40^\circ\text{C}$ ) and high temperature ( $250^\circ\text{C} \leq T \leq 720^\circ\text{C}$ ) conditions. For comparison, the theoretical sputtering yield, as predicted by the TRIM.SP computer code [11], is also plotted. A value of 3.32 eV [12] is used for the surface binding energy of beryllium in the calculations.

When the specimen is maintained at room temperature, the measured sputtering yield is in a good agreement with

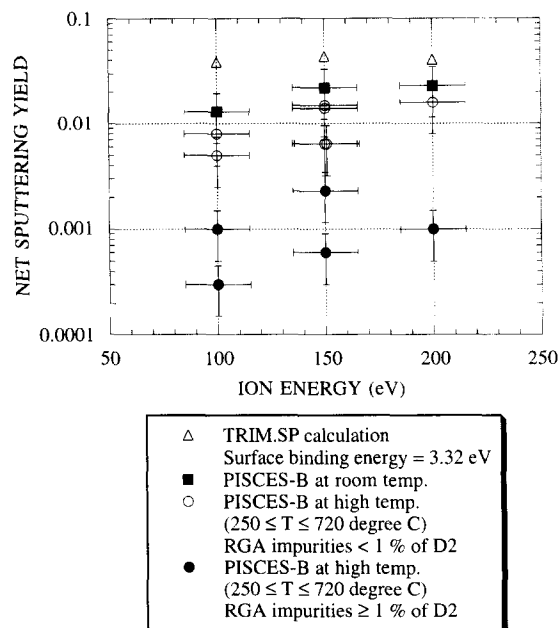


Fig. 1. Measured sputtering yield of beryllium due to deuterium plasma bombardment under different surface temperature conditions. Theoretical sputtering yield of beryllium from the TRIM computer code is also plotted for comparison.

theoretical values within a factor of two. These data also agree with the values measured in an ion beam facility at room temperature within a factor of three [13]. A shiny, eroded metallic surface is revealed after plasma exposure. EDX analysis confirms that the surface is free of impurities except for a trace amount of oxygen. These oxygen species are believed to be (i) impurities in the beryllium specimen existing as BeO [6], and (ii) adsorbed on the specimen surface during the transport in air.

At high specimen temperature, the surface consistently develops a dark gray or black coating within a short period of time [14]. The presence of this film reduces the sputtering yield of beryllium significantly and the film is not removed by extended plasma exposure. From surface analysis, the elements in this layer are identified as carbon, nitrogen, and oxygen. This impurity deposition occurs even when the partial pressure of impurity gases, such as water, carbon monoxide, and hydrocarbons is kept within 1% of the deuterium partial pressure, as monitored by the RGA.

The sputtering yield data at high temperature shown in Fig. 1 are scattered due to the fact that film characteristics, such as elemental composition and film thickness, are affected by the plasma parameters and vacuum conditions. Among the data at elevated temperatures, the higher erosion yield reflects measurements at lower partial pressure of residual gases obtained after extensive plasma discharge cleaning. The data at high temperature are appropriately interpreted as net sputtering yield of mixed-materials, i.e., material composed of beryllium and surface impurities.

The effect of impurity deposition on the erosion of beryllium is dramatically confirmed by monitoring the Be II line intensity [14]. Fig. 2 compares two normalized line intensities, one for a high temperature specimen ( $\sim 640^\circ\text{C}$ ) and the other for a room temperature specimen ( $\sim 40^\circ\text{C}$ ) during plasma exposure. As the specimen is biased negatively, the line intensity increases with enhanced beryllium erosion regardless of the specimen temperature. After this initial increase, the intensity abruptly decreases, suggesting a sudden suppression of beryllium erosion. The line intensity then reaches a steady state. The steady-state intensity at room temperature is about 60% of the initial maximum. Interestingly, at high temperature, the intensity is only about 10% of the initial peak. This implies that at high

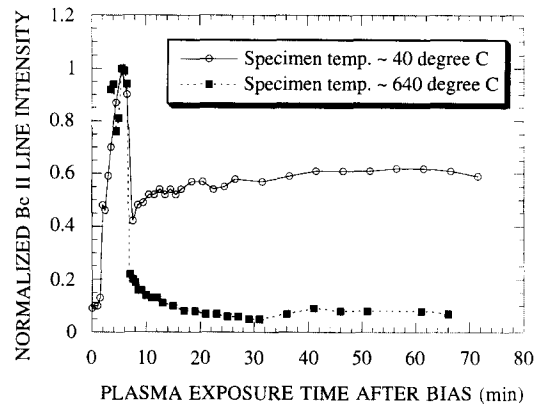
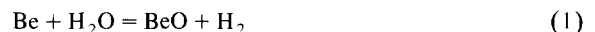


Fig. 2. Comparison of normalized Be II line intensity as a function of plasma exposure time for various specimen temperature conditions.

temperature, a newly formed impurity surface layer shields beryllium and suppresses the erosion process. The sudden change of surface condition is also visually identified by observing the specimen through a viewport. The color of the surface darkens and becomes completely black.

The suppression of the beryllium sputtering yield at high temperature could be explained by a combination of: (i) the surface oxide layer formation due to radiation-enhanced diffusion of bulk beryllium atoms and chemical reactions between beryllium and oxygen-containing molecules; and (ii) the enhanced material mixing between impurity and beryllium atoms, forming a beryllium-impurity mixed surface layer, as confirmed by depth-profile AES analysis. The oxidation of beryllium in dry/moist carbon dioxide and carbon monoxide has been measured by Gregg et al. [15–17] for the temperature range, 500 to  $750^\circ\text{C}$ . In PISCES-B, the oxidation of beryllium and the impurity deposition are attributed to the implantation of ionized oxygen-containing molecules such as  $\text{H}_2\text{O}$  and  $\text{CO}$ . These species are the major residual gases in the PISCES-B vacuum chamber. The growth of the oxide layer on the beryllium surface is governed by the chemical reactions;



As Eq. (2) suggests, incorporation of carbon atoms in the

Table 1

Comparison of the sputtering yield of beryllium measured under various deuterium-plasma bombardment conditions at 150 eV ion bombarding energy in PISCES-B, as well as the theoretical sputtering yield calculated by TRIM.SP

Material	Sputtering yield
Pure beryllium calculated from TRIM.SP code	$4.4 \times 10^{-2}$
Beryllium measured in PISCES-B, when the specimen is kept at room temperature	$2.2 \times 10^{-2} \pm 30\%$
Mixed material measured in PISCES-B, when the beryllium specimen is kept at $500^\circ\text{C}$ (specimen #10)	$2.1 \times 10^{-3} \pm 30\%$ (net erosion)
Beryllium estimated, considering impurity deposition, when the specimen is kept at $500^\circ\text{C}$ (specimen #10)	$6.1 \times 10^{-3} \pm 40\%$

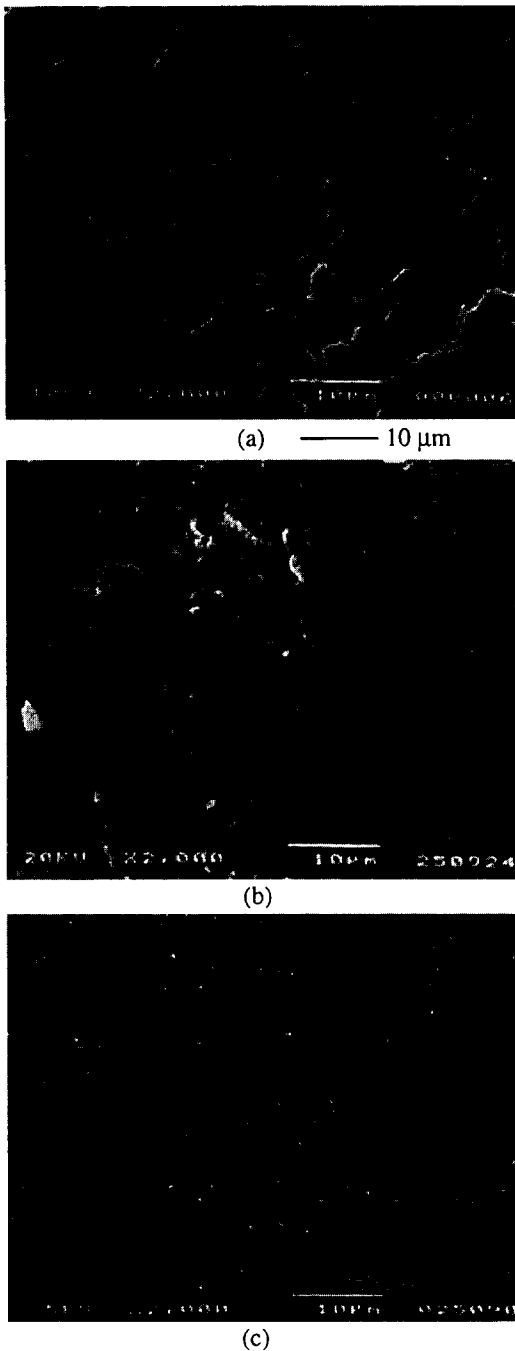
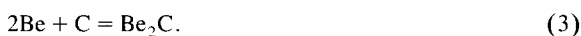


Fig. 3. SEM pictures of various S-65B specimens. (a) As-received. (b) Plasma-bombarded surface with an impurity layer formed during plasma exposure (specimen temp.  $\sim 500^{\circ}\text{C}$ ). (c) Plasma-bombarded, clean, and sputter-etched surface (specimen temp.  $\sim 40^{\circ}\text{C}$ ).

oxide layer is expected. Beryllium carbide can then be formed through



The sputtering yield of beryllium with a mixed-material surface coating requires the estimation of the amount of deposited impurity atoms. One must also account for the fact that a thin impurity layer grows on the surface. The weight gain due to impurity deposition is obtained by integrating the AES data for each impurity species over the total etching time for the specimen, as will be discussed later. We thus correct for the weight of this layer by adding its weight to the measured specimen weight loss. The result is used to calculate the actual sputtering yield of beryllium in the impurity layer. With this correction, we find the beryllium erosion is about 30% of that expected from a room temperature beryllium surface (see Table 1). The table summarizes the sputtering yield of beryllium and of the mixed material by deuterium plasma with ions at 150 eV bombarding energy. The errors in the sputtering yield are calculated from the uncertainties in the measurements.

### 3.2. Surface morphology and characterization

Fig. 3(a) is a SEM picture of an as-received S-65B specimen and shows a coarse surface finish due to machining. Typical SEM pictures of S-65B specimens after deuterium plasma bombardment at different surface temperatures are compared in Fig. 3(b, c). In Fig. 3(b), a rough impurity-deposited surface is shown, which was maintained around  $500^{\circ}\text{C}$ . Fig. 3(c) exhibits a clean surface without any impurity deposition, which was kept at  $40^{\circ}\text{C}$ .

Fig. 4 shows a depth-profile AES result for a specimen which was exposed to a deuterium plasma for 20 min while maintained at a temperature of  $500^{\circ}\text{C}$ . A thin black layer with uniform concentrations of Be, C, N and O is identified. In this layer, the atomic concentration of each impurity species is in the range, 10 to 20%. The thickness of the coating is estimated to be  $\sim 0.2 \mu\text{m}$ . XPS data show that beryllium in the impurity layer is combined with

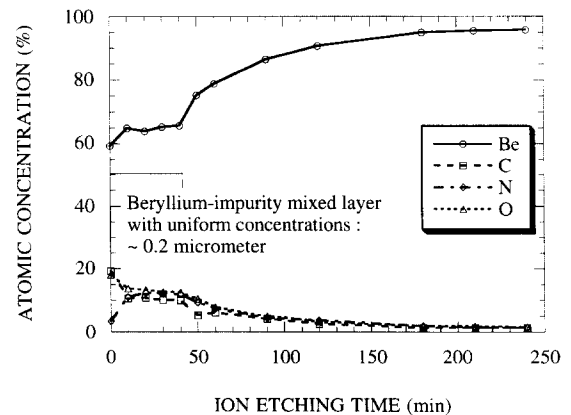


Fig. 4. Elemental composition, from depth-profile AES data (specimen #10), of the impurity layer formed on the beryllium surface at  $500^{\circ}\text{C}$  during deuterium-plasma exposure.

oxygen and forms BeO. Fig. 5(a, b) compare XPS data on the Be 1s spectrum from the same specimen before and after 4 h of Ar beam etching, respectively. It is known that the 1s electron binding energy of pure beryllium is 111.6 eV, while that energy for BeO ranges from 113.5 to 114.2 eV [18]. Only one peak is identified at around 114 eV before the etching, indicating that most beryllium atoms on the surface are combined with oxygen. As the ion beam etching proceeds, another peak is found at around 111.8 eV, clearly marking the change to pure beryllium. The two peaks are separated completely by the end of the etching, as shown in Fig. 5(b). The peak from BeO still exists because the etched area is smaller than the size of X-ray beam.

The formation of Be<sub>2</sub>C in the impurity layer is identified by XPS analysis and data are shown in Fig. 6. The analysis is performed on a specimen, which was maintained at 620°C during the plasma exposure. The figure shows the XPS spectrum from C 1s electron after the specimen is etched by an argon beam for 1 h. Two distinctive C 1s peaks are identified. The large peak occurs

at 284.6 eV, which is a typical C 1s electron binding energy from pure carbon. Another peak is identified at 281.6 eV, which is very similar to the measured C 1s binding energy from Be<sub>2</sub>C by Nieh et al. [19]. The proportion of carbon, which forms Be<sub>2</sub>C, is 26% of all carbon atoms existing in the impurity layer.

An XRD pattern of a beryllium specimen with an impurity coating from plasma exposure at 500°C is shown in Fig. 7. Analysis of the pattern indicates that  $\alpha$ -Be crystallites have the hexagonal lattice parameters with  $a = 2.288 \pm 0.001$  Å and  $c = 3.588 \pm 0.002$  Å, and that the hexagonal BeO is the dominant impurity ( $a = 2.702 \pm 0.005$  Å and  $c = 4.383 \pm 0.009$  Å). The experimentally determined parameters are in good agreement with published values [20]. Additional reflections indicate the presence of other impurities such as the Be<sub>12</sub>Fe-type and Be<sub>3</sub>Fe-type phases. Peak positions for the latter phase suggest that it contains Al. Both of Fe and Al are impurities existing in S-65B beryllium [6]. It should be noted that surfaces of unexposed Be specimens produced essentially similar patterns, so these impurity phases are not associ-

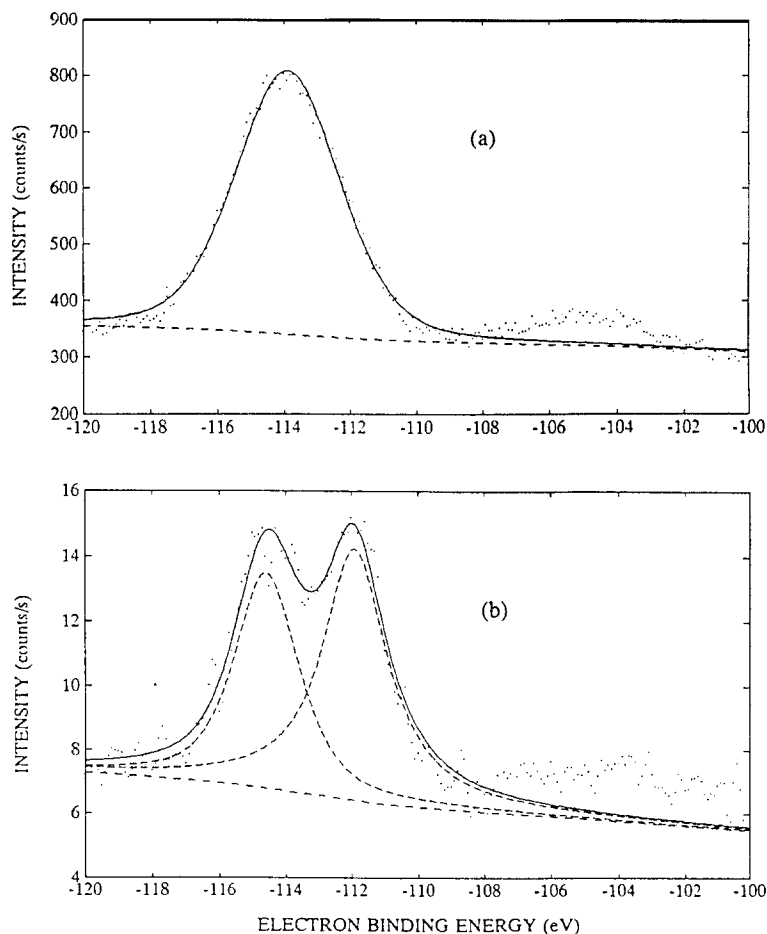


Fig. 5. Be 1s XPS spectra from specimen #10 (a) before and (b) after Ar ion beam etching.

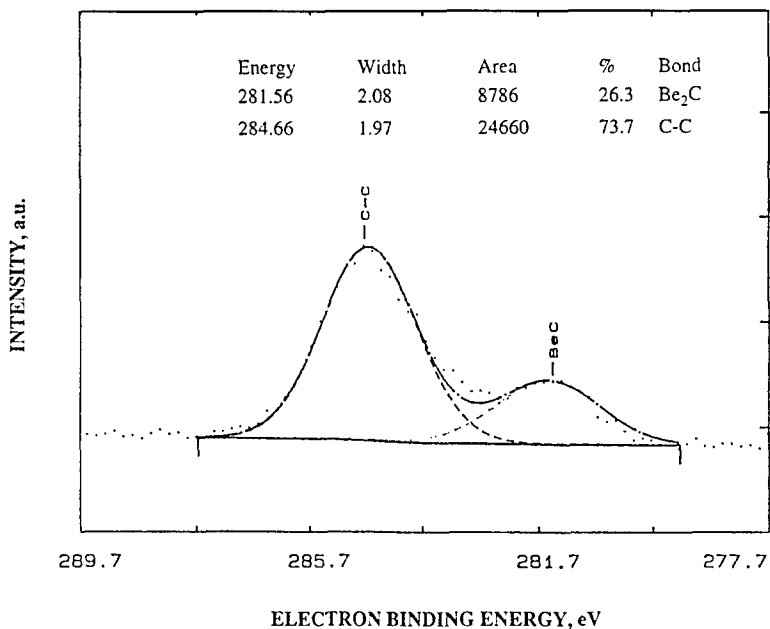


Fig. 6. C 1s XPS spectrum from specimen #11 after 1 h of Ar ion beam etching.

ated with the impurity layer formed during plasma exposure.

The XRD patterns of Be specimen surfaces exposed at high temperature to the plasma show no evidence for the crystalline forms of Be<sub>2</sub>C or carbon. This may be a consequence of an extremely disordered or amorphous structure within the layer. Structural disorder or extremely small crystallites would broaden the impurity reflections and, together with high levels of low atomic number elements, would reduce peak intensities to near background levels.

#### 4. Conclusion

We find that the erosion of beryllium subjected to a high-flux deuterium plasma bombardment in PISCES-B is affected by impurity deposition from residual gases. The surface temperature during plasma exposure and the residual gas pressure in the vacuum chamber are the key parameters controlling the impurity layer formation. At elevated specimen temperatures, plasma impurities with low atomic numbers are deposited on the surface and are not eroded away by extended plasma exposure. This newly formed impurity layer reduces the sputtering yield of beryllium significantly. The reduction of beryllium erosion at high temperature is attributed to (i) a surface oxide layer formation due to radiation enhanced diffusion of bulk beryllium atoms, and (ii) the enhanced material mixing between impurity and beryllium atoms. With this reduced sputtering yield, the lifetime of plasmafacing components using beryllium in fusion devices is expected to increase. By contrast, no impurity deposition is observed when the specimen is maintained at room temperature. In this case, the measured sputtering yield data are in good agreement with theoretical values.

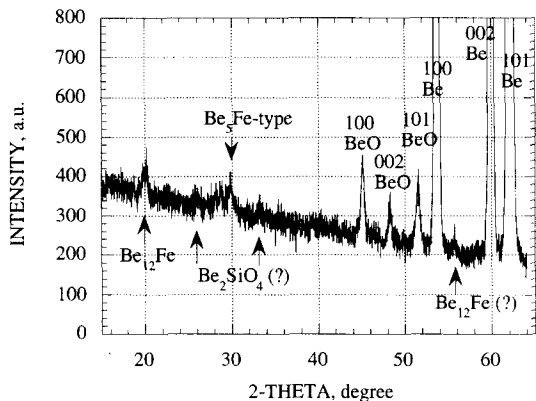


Fig. 7. Typical XRD pattern of S-65B beryllium with an impurity coating after deuterium plasma exposure at 500°C. Pattern obtained using asymmetry geometry (incident angle ~ 1°).

#### Acknowledgements

The authors acknowledge the support of PISCES laboratory staff for their technical assistance. This work is supported by the U.S. Department of Energy under Grant No. DEFG03-86ER-52134.

**References**

- [1] The JET Team, *J. Nucl. Mater.* 196–198 (1992) 3.
- [2] ITER Joint Central Team, *J. Nucl. Mater.* 212–215 (1994) 3.
- [3] J. Bohdansky and J. Roth, *J. Nucl. Mater.* 122–123 (1984) 1417.
- [4] R. Bastasz, *Thin Solid Films* 121 (1984) 127.
- [5] Y. Hirooka, R.W. Conn, T. Sketchley, W.K. Leung, G. Chevalier, R. Doerner, J. Elverum, D.M. Goebel, G. Gunner, M. Khandagle, B. Labombard, R. Lehmer, P. Luong, Y. Ra, L. Schmitz and G. Tynan, *J. Vac. Sci. Technol. A* 8 (1990) 1790.
- [6] G. Petzow, F. Aldinger, S. Jonsson, O. Preuss, in: eds. W. Gerhartz, Y.S. Yamamoto, F.T. Campbell, R. Pfeifferkorn and J.F. Rounsaville, *Ullmann's Encyclopedia of Industrial Chemistry A* 4 (1985) p. 11.
- [7] G.E. Darwin and J.H. Buddeny, *Beryllium* (Academic Press, New York, 1960) p. 237.
- [8] D.M. Goebel, Y. Hirooka, R.W. Conn, W.K. Leung, G.A. Campbell, J. Bohdansky, K.L. Wilson, W. Bauer, R.A. Causey, A.E. Pontau, A.R. Krauss, D.M. Gruen and M.H. Mendelsohn, *J. Nucl. Mater.* 145–147 (1987) 61.
- [9] W.K. Leung, Y. Hirooka, R.W. Conn, D.M. Goebel, B. Labombard and R. Nygren, *J. Vac. Sci. Technol. A* 7 (1989) 21.
- [10] H.P. Summers et al., *Plasma Phys. Controlled Fusion* 34 (1992) 325.
- [11] J.P. Biersack and W. Eckstein, *Appl. Phys. A* 34 (1984) 73.
- [12] C. Kittel, *Introduction to Solid State Physics* (Wiley, New York, 1976) p. 74.
- [13] W. Eckstein, C. Garcia-Rosales, J. Roth and W. Ottenberger, *Sputtering Data*, Max-Planck-Institute for Plasma Physics, IPP 9/82 (February 1993).
- [14] Y. Hirooka et al., *J. Nucl. Mater.* 228 (1996) 148.
- [15] S.J. Gregg, R.J. Hussey and W.B. Jepson, *J. Nucl. Mater.* 2 (1960) 225.
- [16] S.J. Gregg, R.J. Hussey and W.B. Jepson, *J. Nucl. Mater.* 3 (1961) 175.
- [17] S.J. Gregg, R.J. Hussey and W.B. Jepson, *J. Nucl. Mater.* 4 (1961) 46.
- [18] *Handbook of X-ray Photoelectron Spectroscopy* (Physical Electronics Division, Perkin Elmer Corp., Eden Prairie, MN, 1979) p. 34.
- [19] T.G. Nieh, J. Wadsworth and A. Joshi, *Ser. Metall.* 20 (1986) 87.
- [20] JCPDS-International Center for Diffraction Data (Swarthmore, PA, 1989), File Nos. 22-111 and 35-818.